

(version: 2005/ 01 / 07 18 :12 )

# ***Abies* population dynamics simulated by a functional-structural tree model**

Takuya KUBO <sup>\*†</sup> and Takashi KOHYAMA<sup>†</sup>

*Graduate School of Environmental Earth Science, Hokkaido University,  
Sapporo 060-0810, Japan; <sup>†</sup> Frontier Research Center for Global Change,  
Japan Agency for Marine-Earth Science and Technology, 3173-25 Showamachi,  
Kanazawa-ku, Yokohama City, Kanagawa 236-0001, Japan*

(Section and subsection numbers are added just for showing nested structure)

(submitted to *Ecological Research* on 15 September 2004)

---

\*For correspondence. e-mail: [kubo@ees.hokudai.ac.jp](mailto:kubo@ees.hokudai.ac.jp); facsimile: +81.11.706.4954

# 1 Abstract

2 A functional-structural model, **PipeTree**, based on *Abies* population data is developed  
3 to reveal the interaction among processes at physiological, individual and population  
4 scale. Referring field measurements obtained in a comprehensive series of research on  
5 *Abies* forest stand on Mt. Shimagare during 1950s-1980s, we design the structural  
6 components and physiological process models for **PipeTree**. The results of **PipeTree**  
7 simulation support the feasibility of using functional-structural tree model to evaluate  
8 ecosystem performance at stand level. **PipeTree** generates patterns similar to those  
9 in real subalpine forest such as diameter-height relationship and time change in basal  
10 area. After checking the validity of the dynamics of **PipeTree** population, we apply a  
11 sensitivity analysis called  $P_{\max}$  enhancement situation in which the maximum photo-  
12 synthetic rate ( $P_{\max}$ ) of **PipeTree** foliage is increased by 50% (caused by, for example,  
13  $\text{CO}_2$  enrichment). The results of  $P_{\max}$  enhancement simulation show that the increment  
14 by 50% in  $P_{\max}$  makes the doubling of net primary production (NPP) in **PipeTree**  
15 stand. These results suggest the importance of canopy structure in evaluating the  
16 function of terrestrial ecosystem.

17 **Keywords:** functional-structural model, pipe model, resource allocation, water con-  
18 ductance, *Abies veitchii*.

# 1 Introduction

Mathematical modeling of plant and plant population to study the relationship between their function and structure has long history. The basic philosophy in the methodology has been still remained the same as the pioneering work, Monsi and Saeki (1953) that proposed the possibility of mathematical modeling the interaction between plant and light environment. The implementation of plant model, however, has been going through changes over the half century.

One of the first attempt to evaluate plant function in three dimensional space is done by Oikawa and Saeki (1977), a straightforward extension of Monsi-Saeki model. After Takenaka (1994) introduced a branching structure of shoots in the world of plant production model, the spatial configuration of foliage has been risen to a requirement to evaluate the vegetation function. Takenaka's framework also includes that the plant structure is modified by local physiological activities, for example, pruning-up process that the shoots shaded by others are eliminated due to the lack of available resource. Recently, such family of plant models with explicit spatial structure and physiological details are called "functional-structural model" (FSM; Sieväen et al. 2000). One of the successful FSM is LIGNUM (e.g. Sieväen et al. 1997; Perttunen et al. 1998), that is designed as a generic tree simulator. At this moment, the model is used to reproduce realistic shoot-branching architecture under some physiological and morphological con-

1 straits rather than the evaluation of vegetation productivity of the scale larger than  
2 individual.

3 On the other hand, to respond the demand of the age of global change issue, scientists  
4 have developed “big-leaf” models with no detail of vegetation canopy, that is, much  
5 simpler than Monsi-Saeki model. However, Raulier et al. (1999) (who improved the  
6 simplified model by introducing multi-layer structure) points, big-leaf models are widely  
7 used due to two major reasons: ease in parameterization with leaf-level photosynthetic  
8 measurements and tractability in mathematics. In the world of big-leaf models, a single  
9 big leaf is enough to evaluate the ecosystem function of a forest.

10 Although all above tells us, superficially, that we have a segregation between very  
11 simplified models for global change issue and “virtual plant” (Roux et al. 2001) with  
12 spatial details. This is not always true, because some global change models incorpo-  
13 rating spatial structure has arisen in recent years. As the importance of vegetation  
14 structure such as spatial configuration of foliage is accepted, one dimensional or size  
15 structured model plant production models have been developed. (Raulier et al. 1999;  
16 Sitch et al. 2003; Ito and Oikawa 2002) to taking into account the effects of spatial  
17 configuration of vegetation.

18 One dimensional model works to put vertical profile of vegetation, but it is also  
19 true that the models averaging horizontal heterogeneity of sessile organism population

1 generate biased results. In order to adjust the biasness, an approximated method  
2 with stand age distribution (Kohyama 1993; Hurtt et al. 1998; Moorecroft et al. 2001;  
3 Bugmann 2001) has been developed. Whereas the approximation with taking into  
4 account stand age is effective to represent the spatial correlation between the upper  
5 and lower part of stand, the result depends on a parameter of the height vertically  
6 dividing a forest into canopy and others. To minimize vagueness in calculation, we  
7 would conclude the direct method including explicit vegetation structure is the most  
8 persuasive way of investigation in spite of the huge amount of calculation.

9 In the present study, we address a feasibility study of using FSM of tree as a tool to  
10 connect physiological and ecological processes with explicitly spatial structured model.  
11 Firstly, we calibrate our process models and parameters such that the tree model  
12 simulates the real one observed in research plot. This is for the scaling up from shoot  
13 to whole individual level. The next step is the examination of the scaling up from tree  
14 to population whether density depending responses such as morphological changes in  
15 canopy of trees and self-thinning can be derived from the interaction in the ensemble of  
16 the simulated trees. Finally, the changes in ecosystem functional responses are inferred  
17 by a sensitivity analysis for the simulated forest stand.

## 2 Field measurements and outline of PipeTree

In order to integrate physiological and ecological processes within a forest stand with three dimensional structure, **PipeTree** is developed as a dynamical functional-structural model (Sieväen et al. 2000; Roux et al. 2001). The model is specialized to simulate a conifer, in particular, *Abies veitchii* based on the classical and intensive research series on the subalpine forest on Mt. Shimagare during 1950s and 1980s (e.g. Kuroiwa 1960; Kimura et al. 1960; Kohyama 1980; Kohyama and Fujita 1981; Kohyama et al. 1990). The comprehensive set of investigation including from physiological data to community dynamics meets our objective to construct a detailed model that can reveal the interaction of biological process at different levels.

From the first report on the wave regeneration of *Abies* on Mt. Shimagare (Oshima et al. 1958), various types of ecological researches are done around the research plot. As the number of the Shimagare papers is too large to introduce all here, we are only focusing on the references which mainly contributes to the development of **PipeTree**. Kohyama and Fujita (1981) and Kohyama et al. (1990) reveals the forest structure at small stand level in which *Abies veitchii* and *Abies mariesii* build approximately even-aged and even canopy height community. These papers are major references for population structure and time change of **PipeTree** stand. The information at shoot level are obtained from Kohyama (1980) showing the details of shoot habit of *Abies*.

1 The data on physiological processes and matter production of *Abies* are based on  
2 Kuroiwa (1960) and Kimura et al. (1960), respectively.

3 These references suggest that, as a modeling subject, the observation data of crowded  
4 *Abies* stands on Mt. Shimagare possess some advantages than others. As the species  
5 diversity of the forest is very low, we can focus on the most dominant tree species for  
6 our modeling. Although the fraction of *Abies mariesii* in *Abies* stand is not negligible,  
7 we choose the most dominant species, *Abies veitchii* (hereinafter, just *Abies*) as our  
8 modeling target in the study.

9 The data of the subalpine forest of the wave regeneration plot has two major conve-  
10 nient characteristics for our modeling: coherent in tree age within a stand and simplified  
11 structure of individual trees. As Kohyama and Fujita (1981) set several plots along  
12 the stages of the wave regeneration slope and detected the stand age for each plot, the  
13 time change data of stand structure is available. As mentioned in Kohyama (1980),  
14 the architectural structure of *Abies* is simple.

15 Taking these advantages of the characteristics of field measurements for the devel-  
16 opment of `PipeTree`, we also pay attention to keep generality in `PipeTree` design by  
17 partitioning the computer program modules for each biological functions. `PipeTree` is  
18 an *Abies* tree simulator with continuous three dimensional space and discrete timestep  
19 (one year) change. `PipeTree` is named after “pipe model” (Shinozaki et al. 1964a,b),

1 because one of morphological constraints of `PipeTree` is the conservation law of cross  
2 sectional area of stem as described in the section of functional design of `PipeTree`.  
3 The details of `PipeTree` are described in the following sections, but it is impossi-  
4 ble to explain all information in the source code of `PipeTree` because of limitation  
5 of space. The source code which is written mainly in C++ can be downloaded at  
6 <http://hosho.ees.hokudai.ac.jp/~kubo/pipetree/v2004/>. It gives more detailed  
7 reference for the model.

### 8 **3 Structural components of PipeTree**

9 The `PipeTree` consists of two types of component: above- and below-ground part. Each  
10 part can be divided into unit modules which virtually meets the four requirements for  
11 an idealized elementary unit (IEU) proposed by Sieväen et al. (2000). The requirements  
12 are morphological repetition in tree, local environmental dependency, interacting with  
13 adjacent units and small enough to be assumed that the local environment around it  
14 is homogeneous. We employ the policy that all components in `PipeTree` satisfied the  
15 requirements of IEU, because it is adequate to realize our modeling policy, i.e. tree  
16 development without any “global” control such as an allometric relationship between  
17 tree height and basal trunk diameter.

18 In order to describe the structure of `PipeTree`, we must introduce the terms “class”

1 and “object”. The general term of `PipeTree` and its components are called class. We  
2 have `PipeTree` class for trees, `Stem` class for shoots, `Root` class for below-ground part,  
3 and so on. An instance of class is called an object. For example, a `stem` is an object  
4 of `Stem` class, a `tree` is an object of `PipeTree`. As shown here, the first letter of  
5 class name is upper case, while that of object name is lower case. An operator “.” is  
6 introduced to refer the properties of all `PipeTree` objects. For example, `tree.height`  
7 (cm), `tree.D10` (cm) and `tree.age` represent tree height, trunk diameter at 10% height  
8 and age ( $\in \{0, 1, 2, \dots\}$ ) of `tree`.

### 9 **3.1 Above-ground components**

10 The structure of above-ground part of `PipeTree` is modular. The elementary module  
11 object is called `stem` which has cylindrical shape defined by `stem.length` (cm) and  
12 `stem.diameter` (cm). Fig. 1(A) shows a `Stem` class object of `stem.age = 0` at `tree.age`  
13 `= 0`. Because this special `stem` is the origin of all above-ground part, an alias notation,  
14 `stem0`, would be used to express the original `Stem` object.

15 Cross sectional area of `stem`, `stem.area`, is divided into two region: area of “alive  
16 pipes”, `stem.Aa` and “dead pipes”, `stem.Ad` in terms of pipe model (Shinozaki et al.  
17 1964a,b). Alive pipes transfer water in `tree` while dead pipes lack this function.  
18 Approximately, the area of sapwood and heartwood corresponding to `stem.Aa` and  
19 `stem.Ad`. Additionally, the “surface area” of `stem`, `stem.As` (cm<sup>2</sup>), is defined as its

1 curved surface (excluding base area;  $\text{stem}.A_s = \text{stem.length} \times 2\sqrt{\pi \times \text{stem.area}}$ ).

2 At every simulation time step, new **Stem** objects are generated by **stem** of  $\text{stem.age} =$   
3 1, where  $\text{stem.age}$  is a variable of **stem** which is set zero at new **stem** emergence and be  
4 increased by one at every time step. Let us introduce notations **stemM** and **stemD** for  
5 mother and daughter **Stem** objects, respectively. A **stemM** object has a set of  $\{\text{stemD}\}$ ,  
6 that is written as  $\text{stemM.D} = \{\text{stemD}\}$ . Fig. 1(B) shows the relationship of **stemM** and  
7 **stemD** at the top of **PipeTree** object at  $\text{tree.age} = 10$ .

8 From the relationship of **stemM** and **stemD**, we can define  $\text{stem.type}$  and  $\text{stem.order}$ .  
9 As the branching pattern of *Abies* is monopodial, **stemD** can be classified into two types;  
10 main and sub axes, that is,  $\text{stem.type} (\in \{\text{main}, \text{sub}\})$ . Because the mode of branching  
11 of *Abies* is monopodial, a **stemM** can and must have only single **stemD** of  $\text{stemD.type}$   
12 = **main**. All the remaining **stem** objects are those of  $\text{stemD.type} = \text{sub}$ . The order of  
13 **stem**,  $\text{stem.order} (\in \{0, 1, 2, \dots\})$  is defined as follows,

$$\text{stemD.order} = \begin{cases} \text{stemM.order} & \text{if } \text{stemD.type} = \text{main}, \\ \text{stemM.order} + 1 & \text{if } \text{stemD.type} = \text{sub}. \end{cases}$$

14 As the order of original stem of an individual,  $\text{stem0.order}$  is equal to zero, it is trivial  
15 that the orders of **Stem** objects in trunk are always zero, while those of sub branch are  
16 all larger than zero. Fig. 1(A) and (B) show the order structure of **Stem** objects.

17 Let us introduce another property to distinguish **Stem** class objects. The elongation  
18 direction of **stem**,  $\text{stem.direction} \in \{\text{vertical}, \text{lateral}\}$ , expresses whether the

1 `stem` is a part of main trunk or lateral branch (see Fig. 1(B) and Fig. 2). The recursive  
2 inheritance of `stem.direction` from `stemM` to `stemD` can simply defined as follows,

$$\text{stemD.direction} = \begin{cases} \text{stemM.direction} & \text{if stemD.type} = \text{main,} \\ \text{lateral} & \text{if stemD.type} = \text{sub.} \end{cases}$$

3 All `Stem` class objects of `stem.age < foliage_max_age` (`foliage_max_age` is given in  
4 Table 8) have `stem.foliage`, a set of needles. The shape of `stem.foliage` is cylindrical  
5 surrounding stem modules as a metaphor for the bunch of needles.

## 6 **3.2 Below-ground components**

7 As what we know about the below-ground components of plant is much less than  
8 those of above-ground, the modeling of root inevitably becomes a simplified one. The  
9 below-ground part of `PipeTree` that is prepared only to absorb water from soil is  
10 one layer of grid structure. In other words, two dimensional discrete distribution of  
11 `Root` class objects represent the below-ground part. At each grid, the local density  
12 of `root` is divided into two parts: `root.fine` and `root.woody`. Water absorption of  
13 `PipeTree` at a grid depends on the density of fine root, `root.fine` (g), while woody  
14 root, `root.woody` (g), has no functional contribution virtually in `PipeTree`. `Root` class  
15 object is given the ability of growth and expansion. Density of `root` increases at each  
16 grid point, depending on the `root` density itself and on the the allocation of resource  
17 obtained at above-ground part to below-ground part. `Root` objects of a `tree` can  
18 horizontally expand by increasing their number. Fig. 2 shows an example of `Root`

1 objects of `tree.age = 20`.

## 2 **4 Functional design of PipeTree**

3 During one simulation step, `PipeTree` does the following process: light capture, pho-  
4 tosynthesis, water uptake, water allocation, respiration, allocation of photosynthate,  
5 survival check, shoot formation and diameter growth. They are controlled by the law of  
6 conservation in resource under the constraint of structural and morphological restric-  
7 tion. For an object, the range of resource is restricted by itself and its “descendants”  
8 that is the set of objects existing in its distal direction. Additionally, the shoot forma-  
9 tion of `PipeTree` is controlled by some morphological rules described later. Therefore  
10 resource allocation that violates the rules is not available. In this section, we brief each  
11 process of `PipeTree` in simulated abiotic environment (Table 1).

### 12 **4.1 Light capture and photosynthesis**

13 Total amount of assimilation of `tree` is subject to the light capture at each `stem.foliage`.  
14 In `PipeTree`, every `stem.foliage` of `stem.age = 0` (that is, `Stem` objects at the ter-  
15 minal of branches) have one light sensor set upper side of `stem.foliage` to evaluate  
16 the local light intensity,  $I$  ( $\mu\text{mol PPFD}_2 \text{ m}^{-2}\text{s}^{-1}$ ). To decrease the amount of compu-  
17 tation, the `stem.foliage` objects of `stem.age > 0` refer  $I$  of her youngest descendant  
18 of `stem.type = main`. The local light intensity depends on light distribution of the

1 celestial hemisphere and the distribution of `Stem` objects in the simulated space which  
2 represents within- and between-tree competition for light resource.

3 The method of local light evaluation in `PipeTree` can be compiled into a sort of  
4 “ray-tracing” method developed for computer graphics. This is one of the most popular  
5 method for functional-structural models (e.g. Sieväen et al. 1997; Perttunen et al. 1998)  
6 and for forest simulators (e.g. Pacala et al. 1993, 1996). For each light beam (or “ray”),  
7 a light beam tracing program checks the existence of object intercepting light. In this  
8 model, all `Stem` objects (with and without `stem.foliage`) have the ability to cut light  
9 beam perfectly, that is, one hit kills full light. Local light intensity at each light sensor  
10 is evaluated as the total intensity of all light beams of survived. The directions and  
11 intensity of a light beam is given by a corresponding light source on the hemisphere.  
12 The light sources represent an averaged indirect light in day of which details are shown  
13 in Table 1.

14 Evaluating the local light intensity at every `stem`, all `Stem` class objects estimate  
15 their maximum photosynthetic rate (i.e. without water stress) per second under the  
16 local light intensity  $I$  by applying the non-rectangular hyperbola function (Thornley  
17 1976),

$$A(I) = \frac{fI + P_{\max} - \sqrt{(fI + P_{\max})^2 - 4fIqP_{\max}}}{2q} \quad (1)$$

18 where  $A(I)$  ( $\mu\text{mol CO}_2 \text{ m}^{-2}\text{s}^{-1}$ ) is the photosynthetic rate per second;  $f$  ( $\mu\text{mol CO}_2 \mu\text{mol}^{-1}\text{PPFD}$ )

1 is the coefficient of  $I$ ;  $P_{\max}$  is the maximum rate at light saturation point;  $q$  is the de-  
2 gree of convex. Tables 1 and 2 gives the estimates of parameters of photosynthesis,  
3 and Fig. 3 shows the relationship between light intensity and photosynthetic rate.

## 4 4.2 Water uptake and allocation

5 Realized photosynthetic rate at `stem.foliage` is not only restricted by local light in-  
6 tensity but water availability. We employ a model that assimilation rate is proportional  
7 to the ratio of water uptake to water requirement. This model is equivalent to what  
8 water use efficiency (WUE, appeared in Table 2) is a constant. Therefore, realized  
9 assimilation rate,  $A^*(I)$ , can be derived as  $A^*(I) = A(I) \times \text{stem}.W_u / \text{stem}.W_r$  where  
10  $\text{stem}.W_u$  ( $\text{g s}^{-1}$ ) is water uptake rate;  $\text{stem}.W_r$  ( $\text{g s}^{-1}$ ) is the required water given  
11 by  $A(I) / \text{WUE}$  from the definition of WUE. The modification to  $A(I)$  is interpreted  
12 that the realized photosynthetic rate  $A^*(I)$  is limited both by available amount of light  
13 and water at a foliage. The multiplication factor of water,  $\text{stem}.W_u / \text{stem}.W_r$  is equal  
14 to or smaller than one, because the water uptake  $\text{stem}.W_u$  is always less than water  
15 requirement  $\text{stem}.W_r$ . This depends on the water absorption process described in the  
16 following.

17 The total water requirement of `tree` is evaluated by a recursive procedure to sum up  
18 whole  $W_r$  of `stem` objects. Suppose `stemM` is a mother stem and `stemM.D = {stemD}`

1 is the set of all daughters of **stemM**. The total requirement of

$$\mathbf{stemM}.W_r = \mathbf{stemM}.\mathbf{foliage}.W_r + \sum_{\mathbf{stemD} \in \mathbf{stemM}.\mathbf{D}} \mathbf{stemD}.W_r,$$

2 where  $\mathbf{stemM}.\mathbf{foliage}.W_r$  (g) is the water requirement of **stemM.foliage** given by  
3  $A(I)/\text{WUE}$ .

4 Let us illustrate the outline of water capture and allocation in **PipeTree**. The total  
5 amount of captured water by a **tree** depends on the area and density of **root** objects.  
6 The volume taken by a **tree** is the summation of each water absorption by **root** object.  
7 At each grid point, **root** objects from separate **tree** objects compete in water against  
8 each other. The take of each **root** object is proportional to the local density (biomass)  
9 of **root** and total  $W_r$ . The water capture process at below ground part determines the  
10 total amount of water which can be used by a **tree**. The parameter values for water  
11 distribution are described in Table 3.

12 The basic rule for water distribution in **PipeTree** is simple: proportional division,  
13 that is,  $\mathbf{stem}.W_u$  is proportional to the product of  $\mathbf{stem}.W_r$  and water uptake rate of  
14 **tree**,  $\mathbf{tree}.W_u$  ( $\text{g s}^{-1}$ ). The water allocation to **stemD** is,

$$\mathbf{stemD}.W_u = \mathbf{stemM}.W_u \times \frac{\mathbf{stemD}.W_r}{\mathbf{stemM}.\mathbf{foliage}.W_r + \sum_{\mathbf{stemD} \in \mathbf{stemM}.\mathbf{D}} \mathbf{stemD}.W_r}.$$

15 The procedure is applied recursively until the  $\mathbf{stem}.W_r$  for all **stem** objects is evaluated.

16 The procedure of water distribution derives simultaneously the distribution of water

1 potential for all `Stem` objects. The water potential of each `stem`, `stem.Psi` is recursively  
2 defined in direction from root to terminal. From the definitions of alive and dead area  
3 of `stem`, only `stem.Aa` contribute to water distribution. The recursive formulas to  
4 calculate `stem.Psi` are,

$$\text{stemD.Psi} = \text{stemM.Psi} + c_g \Delta H + \frac{E \times \text{stemD.length}}{k_s \times \text{stemD.Aa}}, \quad (2)$$

$$\text{stem0.Psi} = \Psi_{\text{soil}} + \frac{E}{k_r} + \frac{E \times \text{stem0.length}}{k_s \times \text{stem0.Aa}}, \quad (3)$$

5 where  $\Delta H$  (cm) is the difference in height between `stemD` and `stem`;  $E$  ( $\text{g s}^{-1}$ ) is the  
6 flux of water in `stemM`;  $c_g$  ( $\text{MPa cm}^{-1}$ ) is a constant of the effect of gravity;  $k_s$  and  $k_r$   
7 ( $\text{MPa}^{-1} \text{cm}^{-1} \text{g}^{-1} \text{s}^{-1}$ ) are the conductance constants for `Stem` and `Root` respectively;  
8  $\Psi_{\text{soil}}$  (MPa) is water potential of soil. These functional models are developed with  
9 referring the modeling of hydraulic constraints in Magnani et al. (2000). In Table 4,  
10 the values of these parameters are shown.

### 11 4.3 Respiration and photosynthate allocation

Photosynthate at each `stem` is changed into the annual surplus production (Saeki 1960)  
and is transferred to other parts in `tree`. The surplus production of `stem`, `stem.P(I)`  
( $\text{g year}^{-1}$ ), is defined as,

$$\text{stem.P}(I) = (\text{stem.A}^*(I) - r_f) \times C_{A \rightarrow M} \times \text{stem.weight}, \quad (4)$$

1 where  $\mathbf{stem}.A(I)$  is the  $A(I)$  of  $\mathbf{stem}$ ;  $C_{A \rightarrow M}$  is a conversion constant from ( $\mu\text{mol CO}_2 \text{ m}^{-2}\text{s}^{-1}$ )  
2 to ( $\mu\text{mol CO}_2 \text{ g}^{-1}\text{year}^{-1}$ ). In the next step, all photosynthate is recursively transferred  
3 to the direction of mother  $\mathbf{stem}$  with consuming photosynthate for the respiration on  
4 the spot,

$$\begin{aligned} \mathbf{stem}.R_{\max} &= \mathbf{stem}.P(I) + \sum_{\mathbf{stemD} \in \mathbf{stem.D}} \mathbf{stemD}.R, \\ \mathbf{stem}.R &= \mathbf{stem}.R_{\max} - r_s \mathbf{stem}.A_s, \end{aligned}$$

5 where  $\mathbf{stem}.R_{\max}$  is the maximum amount of photosynthate for the respiration of  $\mathbf{stem}$ ;  
6  $\mathbf{stem}.R$  is the residual resource after  $\mathbf{stem}$  consume photosynthate for the respiration  
7 of  $\mathbf{stem}$ ;  $r_s$  ( $\text{g cm}^{-2}$ ) is the coefficient of stem respiration. The estimate for  $r_s$  is shown  
8 in Table 2. The photosynthate virtually lumped together is the resource to grow up  
9 and construct the above- and below-ground part of PipeTree.

10 The model for photosynthate allocation between above- and below-ground part is  
11 plastic and adaptive. The amount of allocation to below-ground part increases under  
12 the condition that total water demand of above-ground part is larger than total water  
13 uptake, while it decreases if water uptake is excess. We adopt the following functional  
14 form to determine the fraction of photosynthate for Root objects,  $u_{\text{new}}$ , which depends  
15 on water requirement and uptake for the origin stem (*i.e.*  $\mathbf{stem0}.W_r$  and  $\mathbf{stem0}.W_u$ )

1 and previous fraction  $u$ :

$$u_{\text{new}} = \frac{1}{1 + \exp[-(\text{stem0}.W_r/\text{stem0}.W_u + \log u - \log(1 - u) - 1)]}. \quad (5)$$

2 The functional form is shown in Fig. 4. As defined in the equation, the below-ground  
3 fraction does not change (*i.e.*  $u_{\text{new}} = u$ ) if  $\text{stem0}.W_r$  and  $\text{stem0}.W_u$  are equivalent.

#### 4 4.4 Survival check

5 The mortality process of **Stem** is one of the most difficult but important part of  
6 **PipeTree**. As having no information on the event, we employ one of the simplest  
7 model that the annual mortality of each **stem** is independently (*i.e.* no correlation  
8 with other objects) determined only by  $\text{stem}.R_{\text{max}}$  defined in the previous subsection,  
9 which is interpreted as the maximum amount of photosynthate for the respiration of  
10 **stem**. The functional form is,

$$\text{stem.mortality} = \exp(-\text{c.mortality} \times \text{stem}.R_{\text{max}}),$$

11 where  $\text{c.mortality}$  is the coefficient of mortality rate (see Table 6). At every time  
12 step (one year) for each **stem** in **tree**, the alive status,  $\text{stem.alive} (\in \{\text{TRUE}, \text{FALSE}\})$ ,  
13 is evaluated by the Bernoulli process of  $\text{stem.mortality}$ .

14 After ending the procedure of checking **stem** survival, we recursively apply a function  
15 that the alive status of daughter stem ( $\text{stemD.alive}$ ) is changed by that of mother's  
16 ( $\text{stemM.alive}$ ). This simulates the death of basal part of a branch or a tree kills its

1 whole terminal part. The value of `stem.alive` is recursively evaluated from `stem0`  
2 (the origin stem of `tree`), that is, `stemD.alive = FALSE` if `stemM.alive = FALSE`. It  
3 is trivial that `stem0.alive = FALSE` indicates that the death of the `tree`.

#### 4 **4.5 Shoot formation and diameter growth**

5 The formation of shoot module (that is, `stem` with `stem.foliage`) requires `PipeTree`  
6 to solve several equations that seek the consistent allocation of photosynthate under  
7 morphological constraints. The process can be divided into three steps: setting number  
8 of the `Bud` class objects for main and sub axis, evaluating scores for all `Bud` and `Stem`  
9 objects and allocating photosynthate between newly created shoots and radial growth  
10 of preexisting `Stem` objects. Implicit numerical solvers are developed to find the best  
11 allocation between elongating of branch and radial growth of supporting part.

12 Branch number of `stem` depends just on `stem.length` as shown in Fig. 5. This is  
13 equal to the number of `Bud` objects, primordiums of `stem`, in `PipeTree`. These `Bud`  
14 objects have `type` ( $\in \{\text{main, sub}\}$ ) property as well as `Stem` object. The set of `Bud`  
15 objects of a `stem` includes one `bud` of `bud.type = main`. The branching angle for each  
16 `Bud` shown in Table 5 depends on `bud.type`.

The angles of newly created `Stem` objects are given by the angles of “modifiers” in  
Table 5 with applying `rotate` function. The `rotate` function is defined as follows

(Fig. 6). First of all, the angles in the global polar coordinates of a daughter **stem** are given as a copy of those of mother **stem**. Let us represent it as **s** that is a set of azimuth angle ( $\mathbf{s}.\theta$ ) and elevation angle( $\mathbf{s}.\phi$ ). The sets of angles shown in Table 5 are called modifiers represented as **m**. Both of **s** and **m** are unit vectors in three dimensional space. To modify **s** by **m**, we prepare two additional unit vectors, **v1** and **v2**, defined as,  $(\mathbf{v1}.\theta, \mathbf{v1}.\phi) = (\mathbf{s}.\theta, \mathbf{s}.\phi + 0.5\pi)$  and  $(\mathbf{v2}.\theta, \mathbf{v2}.\phi) = (\mathbf{s}.\theta + 0.5\pi, 0)$ , respectively. The rotation of **s** can be done by the following procedures (see Fig. 6):

$$\mathbf{s}' = \sin(\mathbf{m}.\phi) \cdot \mathbf{s} + \cos(\mathbf{m}.\phi) \cdot [\sin(\mathbf{m}.\theta) \cdot \mathbf{v1} + \cos(\mathbf{m}.\theta) \cdot \mathbf{v2}],$$

1 where  $s'$  is the vector of rotated. The angles of **s** are fixed once after the values are  
 2 set.

3 The next step of allocation procedure is “scoring” of **stem** and **bud** done by the  
 4 equations and parameters in Table 6. These scores represent the relative intensity of  
 5 sink function. The score of **stem** is proportional to the product of photosynthetic rate  
 6 of **stem** and value from a decreasing function of **stem.order**. The factor of **stem.order**  
 7 is a model of the apical dominance in **PipeTree**. On the other hand, the scoring of **Bud**  
 8 objects must be taken the apical dominance on shoot level into account. In *Abies*, it is  
 9 well known that resource allocation between main and sub axes is changed depending  
 10 on local light environment (Kohyama 1980). Kohyama (1980) reports that the crown  
 11 of *Abies* becomes “umbrella-shaped” under dense canopy (i.e. dark environment).

1 This can be explained by the change in apical dominance of the leader shoot of an  
2 individual tree. In order to simulate the response to light, we introduce an allocation  
3 rule depending on local light intensity shown in Fig. 7. The allocation to main axis of  
4 vertical branch (trunk) extremely decreases in dark condition, whereas less plasticity  
5 to light is assumed for horizontal branch.

6 The final step of shoot formation is photosynthate allocation under morphological  
7 constraints. There are two level competitions in photosynthate; among **Stem** objects  
8 in **tree** and among **Bud** objects in **stem**. As mentioned above, the scores for each  
9 **Stem** and **Bud** objects represent the intensity of sink, that is, the amount of allocated  
10 photosynthate to an object is proportional to the score of the object. The allocation is  
11 under the law of conservation of photosynthate mass. The another type of constraint  
12 for photosynthate allocation is morphological rules. At **Stem** level, the rule of pipe  
13 model (Shinozaki et al. 1964a,b) is applied such that the law of conservation in the  
14 total area of **stem** before and after branching is satisfied at every branching point in  
15 **tree**. In order to check whether the pipe model rule meets at all branching points, the  
16 diameter of newly created **Stem** objects under given photosynthate must be specified.  
17 As we guessed the relationship between length and diameter of **stem** shown in Fig. 8 and  
18 Table 8 with refereeing some literatures such as Kohyama (1980) and the parameters  
19 for needle foliage in Table 8, the diameter of newly created **stem** under given amount

1 of photosynthate can be calculated by implicit numerical method. Taking into account  
2 everything mentioned above, the consistent allocation of photosynthate for every time  
3 step is established by a trial and error method of numerical calculations.

## 4 **5 Simulation Procedure**

5 We drive `PipeTree` simulator under three types of situations: single tree, stand and  
6  $P_{\max}$  enhancement. In the single tree situation, a `PipeTree` object grows up from a  
7 single `stem` and `root`. Virtually no spatial limitations exist. This is done to calibrate  
8 parameters of `PipeTree` by comparing the data of single isolates *Abies* observed around  
9 Mt. Shimagare.

10 After the parameter calibration, the simulation of `PipeTree` population including 30  
11 individual “clones” is driven under the stand situation. The area of simulation plot is  
12 approximately 10 m<sup>2</sup> (3.2 m × 3.2 m quadrat) as described in Table 1. The distribution  
13 of individuals is random on 10 cm grid points. The range of difference in age among  
14 individuals is 20 years, that is, all `Tree` objects gradually appear until the first 20  
15 simulation step. The age distribution is uniform. The configuration of `tree.age = 0`  
16 is the same as that of single tree situation. The stand situation is done to examine  
17 whether the characteristics of *Abies* population observed on Mt. Shimagare can be  
18 generated by the population of `PipeTree` that is not modified in parameters obtained

1 in the single tree situation. For simplicity (and economical issue in calculation), we  
2 remove `PipeTree` objects that can not grow in height during simulation run. This rule  
3 can be translated as a `tree` that lose its “leader shoots”, that is, the `stem` at top of the  
4 `tree` (in other words, `stem` of `stem.type = main` and `stem.order = 0` and `stem.age`  
5 `= 0`).

6 The final procedure,  $P_{\max}$  enhancement situation is almost the same as the stand  
7 situation except increasing by 50% in the maximum photosynthetic rate,  $P_{\max}$  in Eq.(1),  
8 caused by, for example,  $\text{CO}_2$  enrichment for all individuals. This is done to evaluate  
9 the feasibility of using the functional-structural model with ecological details under  
10 changing environment.

## 11 **6 Simulation Results**

12 The snapshots of simulation on the way are shown in Fig. 9. Under stand situation  
13 (Fig. 9(B)), the pruning up of canopy is observed, whereas the `tree` under single  
14 situation (Fig. 9(A)) generates conic canopy with no pruning up of lower branches.

15 The result for single tree situation is shown in Fig. 10 with the data of single isolated  
16 tree on dwarf-bamboo grassland around Mt. Shimagare plot. The trunk diameter (ap-  
17 peared in the result section) is measured at 10% height of tree both in field observation  
18 and simulation. This indicates that the set of parameters for `PipeTree` in tables is one

1 of candidate to reconstruct the trunk diameter-height relationship.

2 The results for stand situation (and the field measurements that corresponds to)  
3 is shown in Fig. 11 and 12. The relationship between diameter-height generated by  
4 **PipeTree** population (Fig. 11(B)) is similar to the pattern obtained from field obser-  
5 vation (Kohyama and Fujita 1981; Kohyama et al. 1990) shown in Fig. 11(A) on the  
6 points that (1) correspondence of diameter-height change to stand age (2) plasticity in  
7 diameter-height relationship under single tree (shown in Fig. 10) and stand situation.  
8 At the same time, we can see some differences in these figures the observed diameter-  
9 height curve in Fig. 11(A) is slightly convex, whereas that of simulated in Fig. 11(B)  
10 is rather concave. The time change of total basal area per land area ( $\text{cm}^2 \text{ cm}^{-2}$ ) of  
11 **PipeTree** stand shown in Fig. 12(A) slightly underestimates than real *Abies* stand  
12 under 40 years, whereas it rather overestimates after 40 years.

13 The results for  $P_{\max}$  enhancement experiment are shown in Fig. 13. Fig. 13(A) can  
14 be interpreted that the increment by 50% in  $P_{\max}$  makes the doubling of net primary  
15 production (NPP) in **PipeTree** stand (baseline represents stand situation). The NPP  
16 of a **tree** is evaluated as the differences of total acquired photosynthesis (gross primary  
17 production) and total respiration. Therefore NPP is equal to `stem0.R` or the mass of  
18 total growth in one year in **PipeTree**. Fig. 13(B) suggests that the doubling in NPP  
19 is due to the doubling in basal area. The enhanced  $P_{\max}$  also accelerates the growth

1 in height. The height growth under  $P_{\max}$  enhancement situation is about 50% faster  
2 than that of baseline.

## 3 **7 Discussion**

4 In the present study, we try to show the feasibility of using functional-structural model  
5 (FSM) to evaluate ecosystem function at stand level. The `PipeTree` simulator gener-  
6 ates patterns similar to what we can observe in the subalpine forest on Mt. Shimagare  
7 such as diameter-height relationship and time change in basal area of stand (Fig. 11 and  
8 12). Shibuya et al. (2004) reports similar patterns in *Abies* stand maintained by wave  
9 regeneration in Hokkaido, Japan to those of Mt. Shimagare. Hence our attempt that  
10 reconstructs *Abies* stand dynamics by modeling could be an approach to understand  
11 something essential for plant population dynamics.

12 By comparing to FSMs already proposed (e.g. Takenaka 1994; Sieväen et al. 1997;  
13 Perttunen et al. 1998; Raulier et al. 1999), `PipeTree` differs on the point that water  
14 availability at every component changes its functional behavior. Through the trial  
15 and error process for `PipeTree` simulation, water dynamics in tree is incorporated to  
16 suppress the growth of terminals, that is, the leader shoots of trunk and branches  
17 when the length of trunk and branches become longer. As dependency on water stress  
18 expressed by water potential ( $\Psi$ ) is consistent to recent studies on tree physiology (e.g.

1 Magnani et al. 2000), we would suggest thus modeling is a natural extension of prior  
2 FSMs and has a potential in scaling-up problems in the field of plant ecosystem.

3 The present simulator provides powerful tool for ecological studies both in individual  
4 and stand scale. In individual scale, it is proved that “whole individual form” or the  
5 allometric relationship between tree diameter and height can be reconstructed by local  
6 interactions of components without any global control. The pattern is a consequence of  
7 the integration of resource competitions and allocation under morphological constraints  
8 and local allometric formulas for the terminal shoot. This could be as well in stand  
9 scale, because the simulated stand is just an ensemble of independent `PipeTree` objects  
10 without any additional special rule for interactions among trees. These discussion could  
11 be concerned with “the problem of pattern and scale in ecology” (Levin 1992). The  
12 scale gaps among shoot, individual tree and population can be connected by computer  
13 intensive methodology.

14 Computer power throws light on multi-scale problems in ecology, but the limitation  
15 of computing still matters. In `PipeTree` simulation, we could increase neither the size of  
16 population nor the number of trials. Although the validity of parameters and process  
17 models must be checked by much more trials of larger populations, it is technically  
18 too hard to do. As the rate-limiting step of `PipeTree` is the estimation of local light  
19 intensity in three dimensional space, which consumes approximately over 95% of total

1 simulation time we may focus on the improvement of the algorithm.

2 All field measurements and biological/ecological information to be embedded into  
3 `PipeTree` is not always sufficiently reliable. One of the most important processes  
4 in `PipeTree` is the probability of death of `stem` (at individual level) and `tree` (at  
5 population level). Whereas the details on survivorship curve for *Abies* has already  
6 been revealed phenomenologically (Kohyama and Fujita 1981), the process models of  
7 mortality in `PipeTree` is far from satisfaction. At shoot level, more detailed research  
8 is required to detect factors controlling shoot mortality, while the pattern of individual  
9 elimination in observed stand data (e.g. Fig. 10(A)) is somewhat enigmatic. The  
10 data suggest that the mortality of *Abies* trees in even-height stand is still high after  
11 60 years from establishment. Although our assumption that `PipeTree` cannot survive  
12 after losing its leader shoot works in this study, more observation on the characteristics  
13 of loser *Abies* in self-thinning stand is needed.

14 The limitation of computer power and available data causes many simplifications  
15 in the modeling of `PipeTree`. As the environment of simulation has no change both  
16 in day and in year, the annual production of `PipeTree` is evaluated as the simple  
17 summation of “average” one second. Although the reproduction of *Abies* could be  
18 considerable important to discuss the problem of resource allocation within tree, we  
19 abandon modeling it due to lack of data. The validation of these simplifications (both

1 by field research and theoretical) would be a worthwhile study for the future.

2 The limitation of computation brings another approximation in the evaluation of  
3 local light environment in PipeTree that the light intensity at current stem is equal  
4 to her mother stem objects. This could induce the overestimation of gross primary  
5 production (GPP) of tree. The effect of the overestimated GPP may be reflected in  
6 time change BA as shown in Fig. 13(B). The results of baseline situation, however,  
7 show no extreme violation from the observation (Fig. 9 - 12). This suggests that we  
8 have another overestimation in mortality or respiration at about and below ground  
9 part.

10 The results obtained under  $P_{\max}$  enhancement situation (Fig. 13) are interesting,  
11 because they suggest the limitation and capability of our approach. The doubling in  
12 net primary production (NPP) by 50% increment in photosynthetic rate (Fig. 13(A))  
13 could be counter-intuitive. Fig. 13(B) gives us a possible explanation that the doubling  
14 of NPP is due to the doubling of basal area (BA) that is nearly proportional to the  
15 amount of needle foliage from the assumption of pipe model (Table 8). This can be  
16 simply explained by total respiration of tree is larger than the half of GPP. The proof  
17 is as follows. What we obtained is,

$$\begin{aligned} \text{NPP} &= \text{GPP} - r && \text{(baseline situation)} \\ 2 \text{ NPP} &= 1.5 \text{ GPP} - (r + \Delta r) && (P_{\max} \text{ enhancement situation}) \end{aligned}$$

18 where  $r$  (kg biomass  $y^{-1}$ ) is total respiration;  $\Delta r$  (kg biomass  $y^{-1}$ ) is increment of

1 respiration under  $P_{\max}$  enhancement situation. Suppose  $r > 0$  and  $\Delta r > 0$ , and these  
2 equations are always true, if  $\Delta r = r - 0.5$  GPP. The difference,  $\Delta r$ , must be positive,  
3 because the supporting part of `tree` increases under  $P_{\max}$  enhancement situation  
4 as shown in Fig. 11(B). For  $\Delta r > 0$ , the condition  $r > 0.5$  GPP is required. We  
5 could, however, doubt whether the doubling NPP is an artifact caused by inadequate  
6 assumptions, because no *Abies* forest of over 1% BA has ever reported in Japan.

7     Considering all above, we would conclude that one of the advantage in using functional-  
8 structural models is the evaluation and validation of “scaling-up” modeling in the field  
9 of plant ecology. Ecologists in the field of tree ecology has proposed many models  
10 which end in each level, such as, physiological, shoot, individual and stand. Such mod-  
11 els could work at the level of interest. We are able to suspect, however, whether these  
12 inconsistency depends on the simplified modeling by neglecting the interactions among  
13 other levels. Suppose we make a phenomenological modeling for *Abies* stand without  
14 physiological and morphological constraints. The modeling must be much easier than  
15 that of `PipeTree`, at the same time, it would be difficult to answer questions on phe-  
16 nomena at different level, such as, the stand dynamics under  $P_{\max}$  enhancement. The  
17 “re-construction” strategy by functional structural has potential to reveal the process  
18 under unobserved situation with checking results by comparing piecemeal knowledge  
19 in physiology and ecology of *Abies*. From the aspect of questing of modeling with

1 few inconsistency, we know this paper is just the start point of modeling *Abies* stand,  
2 hence the further improvement by validation under observed and unobserved situation  
3 should be our future works for PipeTree.

## Acknowledgments

We sincerely thank the following people for their helpful comments and suggestions: Kouki Hikosaka, Kyoko Kato, Tsuyoshi Kobayashi, Takeshi Seki, Testuo Shirota, Akihiro Sumida, Maki Suzuki, Akio Takenaka, Naoaki Tashiro, Kiyoshi Umeki. The development and analysis of PipeTree were done only by free and/or open source software distributed via the internet. We thank and admire those who develop and maintain them. This work was partially supported by a Grant-in-Aid from the Ministry of Education, Culture, Sports, Science and Technology of Japan (No. 15770006).

## References

- Bugmann H (2001) A review of forest gap models. *Climatic Change* 51:259–305.
- Hurtt GC, Moorecroft PR, Pacala SW, Levin SA (1998) Terrestrial models and global change: challenges for the future. *Global Change Biology* 4:581–590.
- Ito A, Oikawa T (2002) A simulation model of the carbon cycle in land ecosystem (Sim-CYCLE): A description based on dry-matter production theory and plot-scale validation. *Ecological Modeling* 151:147–179.
- Kimura M, Mototani M, Hogetsu K (1960) Ecological and physiological studies on the vegetation of Mt. Shimagare VI Growth and dry matter production of young *Abies* stand. *Botanical Magazine, Tokyo* 81:287–296.
- Kohyama T (1980) Growth pattern of *Abies mariesii* saplings under conditions of open-growth and suppression. *Botanical Magazine, Tokyo* 93:13–24.
- Kohyama T (1993) Size-structured tree populations in gap-dynamic forest – the forest architecture hypothesis for the stable coexistence of species. *Journal of Ecology* 81:131–143.
- Kohyama T, Fujita N (1981) Studies on the *Abies* population of Mt Shimagare I. Survivorship curve. *Botanical Magazine, Tokyo* 94:55–68.
- Kohyama T, Hara T, Tadaki Y (1990) Patterns of trunk diameter, tree height and crown depth in crowded abies stands. *Annals of Botany* 65:567–574.
- Kuroiwa S (1960) Ecological and physiological studies on the vegetation of Mt. Shimagare IV Some physiological functions concerning matter production in young *Abies* trees. *Botanical Magazine, Tokyo* 73:133–141.
- Levin SA (1992) The problem of pattern and scale in ecology. *Ecology* 73:1943–1967.
- Magnani F, Mencuccini M, Grace I (2000) Age-related decline in stand productivity: the role of structural acclimation under hydraulic constraints. *Plant Cell and Environment* 23:251–263.
- Monsi M, Saeki T (1953) Über den Lichtfaktor in den Pflanzengesellschaften und seine Bedeutung für die Stoff-produktion. *Japanese Journal of Botany* 14:22–52.
- Moorecroft PR, Hurtt GC, Pacala SW (2001) A method for scaling vegetation dynamics: The ecosystem demography model (ED). *Ecological Monographs* 71:557–586.

- Oikawa T, Saeki T (1977) Light regime in relation to plant population geometry I a monte carlo simulation of light microclimates within a random distribution foliage. *Botanical Magazine, Tokyo* 90:1–10.
- Oshima Y, Kimura M, Iwaki H, Kuroiwa S (1958) Ecological and physiological studies on the vegetation of Mt. Shimagare I Preliminary survey of the vegetation of Mt. Shimagare. *Botanical Magazine, Tokyo* 71:289–301.
- Pacala SW, Canham CD, Silander JAJ (1993) Forest models defined by field measurements: I the design of a northeastern forest simulator. *Canadian Journal of Forest Research* 23:1980–1988.
- Pacala SW, Canham CD, Silander JAJ, Kobe RK, Ribbens E (1996) Forest models defined by field measurements: Estimation, error analysis and dynamics. *Ecological Monographs* 66:1–43.
- Perttunen J, Sieväen R, Nikinmaa E (1998) LIGNUM: a model combining the structure and the functioning of trees. *Ecological Modelling* 108:189–198.
- Raulier F, Berner PY, Ung C (1999) Canopy photosynthesis of sugar maple (*Acer saccharum*): comparing big-leaf and multilayer extrapolations of leaf-level measurements. *Tree Physiology* 19:407–420.
- Roux XL, Lacoite A, Escobar-Gutiérrez A, Dizès SL (2001) Carbon-based models of individual tree growth: A critical appraisal. *Annals of Forest Science* 58:469–506.
- Saeki T (1960) Interrelationships between leaf amount, light distribution and total photosynthesis in a plant community. *Botanical Magazine, Tokyo* 73:55–63.
- Shibuya M, Haga N, Sasaki T, Kikuchi S, Haruki M, Noda M, Takahashi K, Matsuda K (2004) Stand and self-thinning dynamics in natural *Abies* stands in northern Hokkaido, Japan. *Ecological Research* 19:301–309.
- Shinozaki K, Yoda K, Hozumi K, Kira T (1964a). A quantitative analysis of plant form – the pipe model theory I. basic analysis. *Japanese Journal of Ecology* 14:97–105.
- Shinozaki K, Yoda K, Hozumi K, Kira T (1964b). A quantitative analysis of plant form – the pipe model theory II. further evidence of the theory and its application to forest ecology. *Japanese Journal of Ecology* 14:133–139.
- Sieväen R, Nikinmaa E, Nygren P, Ozier-Lafontaine H, , Perttunen J, Hakula H (2000) Components of functional-structural tree models. *Ann. For. Sci* 57:399–412.

- Sieväen R, Nikinmaa E, Perttunen J (1997) Evaluation of importance of sapwood senescence on tree growth using the model LIGNUM. *Silva Finica* 31:329–340.
- Sitch S, Smith B, Prentice IC, Arneth A, Bondeau A, Cramer W, Kaplan JO, Levis S, Lucht W, Sykes MT, Thonicke K, Venevsky S (2003) Evaluation of ecosystem dynamics, plant geography and terrestrial carbon cycling in the LPJ dynamic global vegetation model. *Global Change Biology* 9:161–185.
- Takenaka A (1994) A simulation model of tree architecture development based on growth response to local light environment. *Journal of Plant Research* 107:321–330.
- Thornley JHM (1976) *Mathematical models in plant physiology*. London: Academic Press.

**Table 1** Parameters for simulated environment.

(parameter name)	(value and units)
<code>xyz_min</code>	(-160.0, -160.0, 0.0) (cm)
<code>xyz_max</code>	(+160.0, +160.0, 1500.0) (cm)
(note) These two vectors define the size of simulation plot for stand situation. The boundary planes of $x$ and $y$ are both periodic for light calculation and branch growth. The boundary planes of $z$ is absorption. The periodic boundary plane shifts in parallel to the opposite boundary, while the absorption boundary plane terminates the tracking of light beam. For the simulation of single tree situation, no boundary is assumed.	
<code>I<sub>max</sub></code>	2000 ( $\mu\text{mol PPF D m}^{-2} \text{ s}^{-1}$ )
(note) Maximum PPF D density. The product of <code>I<sub>max</sub></code> and local light intensity (in normalized value in $[0, 1]$ ) is equal to $I$ in Eq.(1) in body.	
<code>n_latitude</code>	9
<code>n_longitude</code>	9
<code>phi_min</code>	$0.1\pi$ (radian)
<code>gradient_factor</code>	3.0
(note) These four parameters define the configuration on light intensity of celestial hemisphere. <code>n_latitude</code> and <code>n_longitude</code> are the partition number in the direction of latitude and longitude of the sky hemisphere. Hence the number of light sources is the product of them. Note that <code>phi_min</code> is the minimum elevation angle of light sources. The normalized intensity of light source are given by <code>gradient_factor</code> that is the relative intensity of light source at the zenith against the point at <code>phi_min</code> . As the light intensity defined so has no bias on the hemisphere, we can interpret it as a simulation of full of diffused light without any direct light.	
<code>precipitation</code>	1000 (mm)
(note) Annual precipitation. We assume that all water fallen in simulation plot can be used by trees.	

**Table 2** Parameters for photosynthesis and respiration. Most of them are used around Eq.(1) in body. The photosynthetic curve determined by these estimates are shown in Fig. 3. The estimates are evaluated from some literatures such as Kuroiwa (1960).

(parameter name)	(value and units)
<code>p_max</code> (note) Maximum photosynthetic rate, $P_{\max}$ in Eq.(1).	8.5 ( $\mu\text{mol CO}_2 \text{ m}^{-2} \text{ s}^{-1}$ )
<code>f</code> (note) The coefficient of light $I$ , $f$ in Eq.(1).	0.05 ( $\mu\text{mol CO}_2 \mu\text{mol}^{-1} \text{ PPFD}$ )
<code>q</code> (note) Degree of non-orthogonality, $q$ in Eq.(1).	0.8 ( $\text{s m}^2 \mu\text{mol PPFD} \mu\text{mol CO}_2^{-1}$ )
<code>assimilation_wp</code> (note) The degree of decreasing in photosynthetic rate by <code>stem.Psi</code> , water potential of <code>stem</code> . The assimilation rate per second, $A(I)$ in Eq.(1) is multiplied by $\exp(-\text{assimilation\_wp} \times \text{stem.Psi})$ .	0.01 ( $\text{MPa}^{-1}$ )
<code>converter</code> (note) This is the constant, $C_{A \rightarrow M}$ in Eq.(4), to covert the assimilation rate per second ( $\mu\text{mol CO}_2 \text{ m}^{-2} \text{ s}^{-1}$ ) annual production rate ( $\mu\text{mol CO}_2 \text{ g}^{-1} \text{ year}^{-1}$ ).	0.21 ( <i>(rightarrow see note)</i> )
<code>respiration_foliage</code> <code>respiration_wood</code> (note) The respiration rate is defined in leaf area based, while the respiration rate of <code>stem</code> ( $r_s$ in body) is proportion to “surface area” of <code>stem</code> ( <code>stem.A_s</code> ) defined in body.	0.85 ( $\mu\text{mol CO}_2 \text{ m}^{-2} \text{ s}^{-1}$ ) $1.1 \times 10^{-2}$ ( $\text{g cm}^{-2} \text{ year}^{-1}$ )
<code>water_use_efficiency</code> (note) The estimate is evaluated from some literatures such as Kimura et al. (1960).	250 ( $\text{g g}^{-1}$ )

**Table 3** Parameters for root class object.

(parameter name)	(value and units)
<code>c_respiration</code> (note) Annual turnover rate of fine root. Here we equate the turnover of fine root with fine root respiration, as both of them consume photosynthate with unknown rate.	0.10 (g g <sup>-1</sup> )
<code>c_water</code> (note) Water uptake rate is proportion to $1 - \exp(\text{c\_water} \times D_r)$ where $D_r$ (gcm <sup>-2</sup> ) is local density of fine root.	7.0 (g <sup>-1</sup> )
<code>c_conversion</code> (note) The conversion coefficient from fine root to woody root.	0.10 (g g <sup>-1</sup> )

**Table 4** Parameters for water conductance. These parameters are appeared around Eq.(2) and (3) and are evaluated from some literatures such as Magnani et al. (2000).

(parameter name)	(value and units)
<code>total_time</code>	$8.21 \times 10^6$ (s)
	(note) Approximated total photosynthetic time during May to October. 12 hours $\times$ 190 days. This value is used in calculation of water requirement per second.
<code>water_potential_soil</code>	-0.5 (MPa)
	(note) Water potential of soil, $\Psi_{\text{soil}}$ in Eq.(3).
<code>const_wp_grav</code>	$9.8 \times 10^{-5}$ ( $\text{cm s}^{-1} \text{kg m}^{-3}$ )
	(note) The effect of gravity, $c_g$ in Eq.(2).
<code>conductance_root</code>	$1.0 \times 10^4$ ( $\text{g g}^{-1} \text{MPa}^{-1}$ )
	(note) The conductance of root, $k_r$ in Eq.(2).
<code>conductance_stem</code>	5.0 ( $\text{m}^2 \text{s}^{-1} \text{MPa}^{-1}$ )
	(note) The conductance of stem, $k_s$ in Eq.(2).

**Table 5** Angles for newly created **Stem** class objects. The set of  $(\theta, \phi)$  represents that of angles of azimuth and elevation.

(parameter name)	(value and units)
<code>modifier_vertical</code>	$(0.75\pi, 0.50\pi)$ (radian)
<code>modifier_lateral</code>	$(1.50\pi, 0.498\pi)$ (radian)
(note) These sets of angles of azimuth and elevation determine the rotation angle between <b>stem</b> of mother and daughter, that is, branching angle of main (non-lateral) shoot. The origin for <b>stemD</b> rotation is the terminal point of <b>stemM</b> . The three dimensional angle for <b>stemD</b> elongation is given by <b>rotate</b> function defined in body.	
<code>branching_vertical</code>	$(-, 0.15\pi)$ (radian)
(note) <code>branching_vertical</code> gives the angles of elevation of lateral branch of the leader shoot of <b>PipeTree</b> . As the angles of azimuth for these lateral shoots depend of the number of them, the angle between two adjacent shoots is always maximized ( <i>e.g.</i> $0.5\pi$ for four lateral shoots).	
<code>branching_lateral</code>	$(0.03\pi, 0.10\pi)$ (radian)
<code>branching_lateral</code>	$(0.97\pi, 0.15\pi)$ (radian)
(note) The branching angles for lateral shoots of horizontal <b>stem</b> are given by these two sets of angles of azimuth and elevation. The former and latter set are corresponding to “right” and “left” branching, respectively.	
<code>branching_range_vertical</code>	$(0.20\pi, 0.02\pi)$ (radian)
<code>branching_range_lateral</code>	$(0.00\pi, 0.05\pi)$ (radian)
(note) These sets of radian indicate the ranges of “noise” in branching angle of azimuth and elevation. The branching angle is the sum of <code>branching_X</code> (X in <code>vertical</code> and <code>horizontal</code> ) and random variable from uniform distribution of range of <code>branching_range_X</code> .	

**Table 6** Parameters for `stem` scoring (for photosynthate competition between terminal `Stem` class objects).

(parameter name)	(value and units)
<code>order_factor</code>	0.15
(note) These two factors are used in score evaluation for each <code>stem</code> . The score is defined as,	
$\text{stem.score} = \text{stem.P}(I) \times \exp(-\text{order\_factor} \times \text{stem.order})$	
where both <code>stem.P(I)</code> and <code>stem.order</code> are annual net production and branch order of <code>stem</code> . Their details are described in body. The functional form of <code>stem.score</code> is determined by a lot of trial and error process. Finally, we adopt the simplest model in which <code>stem.score</code> depends only on <code>stem.order</code> but not on others (e.g. photosynthetic rate and local light intensity).	
<code>dark_inhibition_power</code>	5.0
<code>bud_main_dark_vertical</code>	0.00
<code>bud_main_light_vertical</code>	0.85
<code>bud_main_dark_lateral</code>	0.60
<code>bud_main_light_lateral</code>	0.75
(note) These parameters are used in resource allocation between main and lateral buds for vertical and horizontal <code>stem</code> . Let us suppose $X \in \{\text{vertical, horizontal}\}$ . The fraction to main bud of <code>stem</code> of $X$ is defined as,	
$\frac{\text{bud\_main\_dark\_X} + \text{pow}(L, \text{dark\_inhibition\_power})}{\text{bud\_main\_light\_X} + \text{bud\_main\_dark\_X}}$	
where $\text{pow}(a, b)$ represents $a^b$ ; $L$ is <code>stem.local_light</code> . The fraction change depending on $L$ is shown in Fig. 5.	
<code>c_mortality</code>	$1.5 \times 10^2 \text{ (g}^{-1}\text{)}$
(note) The mortality of <code>stem</code> is defined as $\exp(-\text{c\_mortality} \times \text{stem.resouce})$ .	

**Table 7** Parameters for shoot formation.

(parameter name)	(value and units)
<code>d_length_power</code>	1.1
<code>d_length</code>	62.0 (cm)
<code>c_wp_length</code>	25.0 (MPa <sup>-1</sup> )
<code>wp_length50</code>	-0.59 (MPa)
(note) The length of <code>stem</code> , <code>stem.length</code> is given from the following equation including the above parameters,	
$L = \frac{d\_length}{1 + \exp(-c\_wp\_length(W - wp\_length50))} D^{d\_length\_power}$	
where the parameters in italic, $L$ , $D$ and $W$ , are <code>stem.length</code> , <code>stem.diameter</code> and <code>stem.Psi</code> (water potential), respectively. The length of <code>stem</code> monotonically increases with <code>stem.diameter</code> , and monotonically decrease with <code>stem.Psi</code> , shown in Fig. 7.	
<code>density_wood</code>	0.4 (g cm <sup>-3</sup> )
(note) <code>density_wood</code> , the value (constant for all <code>Stem</code> objects) is determined with referring some literatures such as Kohyama (1980). This is required to evaluate <code>stem.weight</code> from <code>stem.volume</code> .	
<code>pipe_bundle_min_length</code>	0.5 (cm)
(note) The <code>stem</code> of <code>stem.length</code> is smaller than <code>pipe_bundle_min_length</code> is removed before it grows. This is an ad hoc criteria to decrease the number of shoot.	

**Table 8** Parameters for needle foliage.

(parameter name)	(value and units)
<code>area_foliage</code>	25.0 (g cm <sup>-2</sup> )
(note) Here the rule of pipe model (the law of conservation in area) is applied that the amount of needle foliage is proportional to the area of stem. The conversion constant is derived from Kohyama (1980).	
<code>foliage_max_age</code>	3 (year)
<code>needle_cylinder_radius</code>	1.2 (cm)
(note) The value of <code>foliage_max_age</code> is set by referring to Kohyama (1980) in which the age distribution of needles attached to shoot is given. We assume <code>foliage_max_age</code> is a constant as a approximated model of foliage. As mentioned in body, the shape of needle foliage is cylindrical, as an approximation of real needles.	
<code>eye_rotate_vertical</code>	(0.00, 0.50 $\pi$ ) (radian)
<code>eye_rotate_lateral</code>	(0.50 $\pi$ , 0.50 $\pi$ ) (radian)
(note) These sets of angles gives the location of <code>eye</code> , light sensor to evaluate local light intensity at each <code>stem</code> . The first and second values in vector represents angles of azimuth and elevation of <code>eye</code> from the root of <code>stem</code> .	

## Figure Legends

**Fig. 1** Schemata of `Stem` class objects with needle foliage (represented as cylinder).

(A) `stem` of `stem.age = 0`. This is the origin of all `Stem` objects, `stem0`, of an `PipeTree`.

At this age, `PipeTree` consists of a single `stem` with needle foliage (represented as cylinder) with the attached `root` object (represented as ball). The size of a `Stem` class object is characterized by its length (`stem.length`) and diameter (`stem.diameter`). (B)

Top of a `PipeTree` at `tree.age = 10`. Showing the relationship between mother `stem`, `stemM`, and her three daughters, `stemD` objects. The notification of “(vertical)” and “(lateral)” indicates `stem.direction`.

(C) Structural properties of `stem` of `tree.age = 16`: `stem.type` is axis type `{main, sub}`; `stem.order` is branch order `{0, 1, 2, ...}`; `stem.direction` is the direction of shoot elongation in `{vertical, lateral}`; `stem.age` is stem age that is in `{0, 1, 2, ...}`. Note the nested structure of `stem.type`  $\in$  `{main, sub}`.

**Fig. 2** Scheme of `Root` class objects of `tree.age = 20`. An instance of `root` on grid point consists of fine and wood root, represented by balls. The size of ball indicates the local density of root.

**Fig. 3** Photosynthetic curves for `PipeTree`, the functional form is given by Eq.(1). The horizontal axis is local light intensity (in relative value) and the vertical axis is photosynthetic rate ( $\mu\text{mol CO}_2 \text{ m}^{-2}\text{s}^{-1}$ ). Solid and dashed curves correspond to base-

line (maximum photosynthetic rate is equal to 8.5) and  $P_{\max}$  enhancement simulation (12.8), respectively. The estimates for other parameters are shown in Tables 1 and 2.

**Fig. 4** The time change in allocation between above- and below- ground component defined by Eq.(5). Suppose the ratio of below- to above ground is  $u$  at a simulation time step. The horizontal axis is the ratio of water requirement ( $W_r$ ) to realized uptake ( $W_u$ ) under  $u$ . The vertical axis shows the allocation to below-ground at the next step,  $u_{\text{new}}$ . This can be interpreted as  $u_{\text{new}} > u$  if water uptake is insufficient, while  $u_{\text{new}} < u$  under the situation of water excess. Note that the curve defined by Eq.(5) always contains the point  $(1, u)$  for any  $u$ .

**Fig. 5** Relationship between mother `stem.length` and number of buds (or number of daughter `Stem` objects). Solid and dashed curves correspond to vertical and lateral class of `stem`, respectively. The branch number (or number of daughter `stem`) increases as the length of mother `stem` for vertical type, while the possible number of branches is either zero or two for `Stem` objects of `stem.type = sub`. These values are inferred from some literatures such as Kohyama (1980) and Kohyama's field observation around Mt. Shimagare (unpublished data).

**Fig. 6** Polar coordinates to rotate a daughter `stem` attached the top of her mother stem, `0`. The azimuth and rotation angles of an unit vector vector `s` is equal to those of mothers. Vectors `v1` and `v2` are both orthogonal to `s` as defined in body. Given a

modifier defined by  $m.\theta$  and  $m.\phi$ , the rotated vector  $\mathbf{s}'$  is obtained on the coordinates defined by vectors  $\mathbf{s}$ ,  $\mathbf{v1}$  and  $\mathbf{v2}$ .

**Fig. 7** Relationship between local light intensity of `stem` and allocation to “main axis.” The horizontal axis is local light intensity (in relative value) and the vertical axis is the fraction of photosynthate allocation to main axis at new shoot formation. Solid and dashed curves are `vertical` and `lateral` class of `stem`. As photosynthate allocation of *Abies* is changed conditionally with light intensity (Kohyama 1980), we employ a functional form (shown in Table 6) such that the curves in the figure can be generated.

**Fig. 8** Relationship between length and diameter of newly created `stem` depending on water potential at mother stem. We assumed that `stem.length` decreases as the declining of water potential. The functional form and parameter values are shown in Table 7.

**Fig. 9** Three dimensional snapshot of `PipeTree` growth. (A) A `PipeTree` of `tree.age` = 40 grows up under single tree situation. (B) A `PipeTree` stand at simulation timestep 44. Note that the x- and y-boundaries are all periodic.

**Fig. 10** Relationship between tree basal trunk diameter (D) and top height (H) for trees that grow up under single isolated circumstance. The trunk diameter is measured at 10% height of tree both in field observation and simulation. Circles represent field

measurements around Mugikusa Pass near Mt. Shimagare in 1978. Solid curve represent D-H relationship generated by `PipeTree` simulation under single tree setting. Vertical ticks on the curve are shown at every annual observation time. The age of `PipeTree` at right end of the figure is about 50 years old.

**Fig. 11** Relationship between tree basal trunk diameter (D) and height (H) in a dense stand. The diameter is measured at 10% height of tree both in field observation and simulation. Open and closed triangles and circles represent D-H relationship of all trees that live at each observation time; open triangle for stand age 23, closed triangle for 40, open circle for 63 and closed circle for 84. (A) Field measurements from the research of Mt. Shimagare (Kohyama and Fujita 1981; Kohyama et al. 1990). (B) A result of `PipeTree` simulation starting from the population of 30 individuals in 10 m<sup>2</sup> stand.

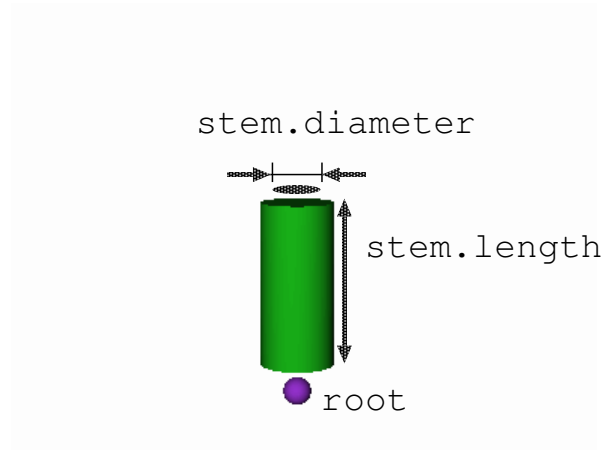
**Fig. 12** Comparison in basal area and tree density change between field measurements and `PipeTree` simulation (one trial). (A) Time change of basal area. Closed circles represents the field measurements on Mt. Shimagare (Kohyama and Fujita 1981). Solid curve represent the result of `PipeTree` simulation. (B) Relationship between total number of `PipeTree` objects in 10 m<sup>2</sup> stand and the total biomass excluding below-ground part of survived trees. Solid curve represents the trajectory of time change in simulation. Closed circles are pointed at every 5 years. Dashed line is attached just for

the reference of “self-thinning” line. The line of equation is  $y = 8.0 \times 10^5 x^{0.5}$  where  $x$  and  $y$  are total number and biomass of trees in simulation plot ( $10 \text{ m}^2$ ), respectively.

**Fig. 13** Results of  $P_{\max}$  enhancement experiment where maximum photosynthetic rate ( $P_{\max}$  in Eq.1) increases by 50% of baseline simulation (see Fig. 3). (A) Time change in net primary production (NPP). Solid and dashed curves correspond to baseline and  $P_{\max}$  enhancement simulation, respectively. (B) Time change in basal area. Closed circles represent the field measurements on Mt. Shimagare (Kohyama and Fujita 1981) as in Fig. 12(A). Dashed curve represents the result of PipeTree simulation under  $P_{\max}$  enhancement situation.

Fig. 1

(A) tree.age = 0



(B) tree.age = 10

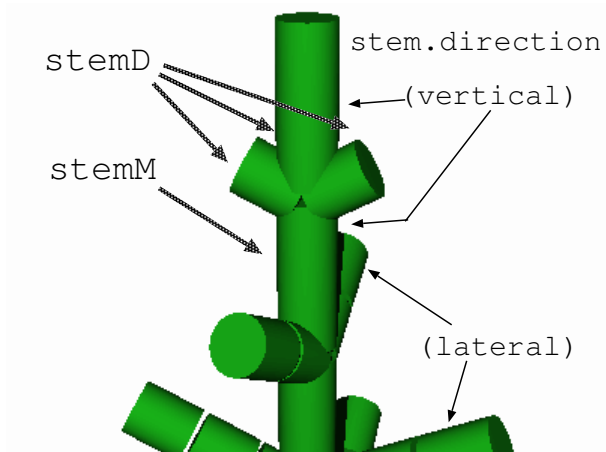


Fig. 1 (continued)

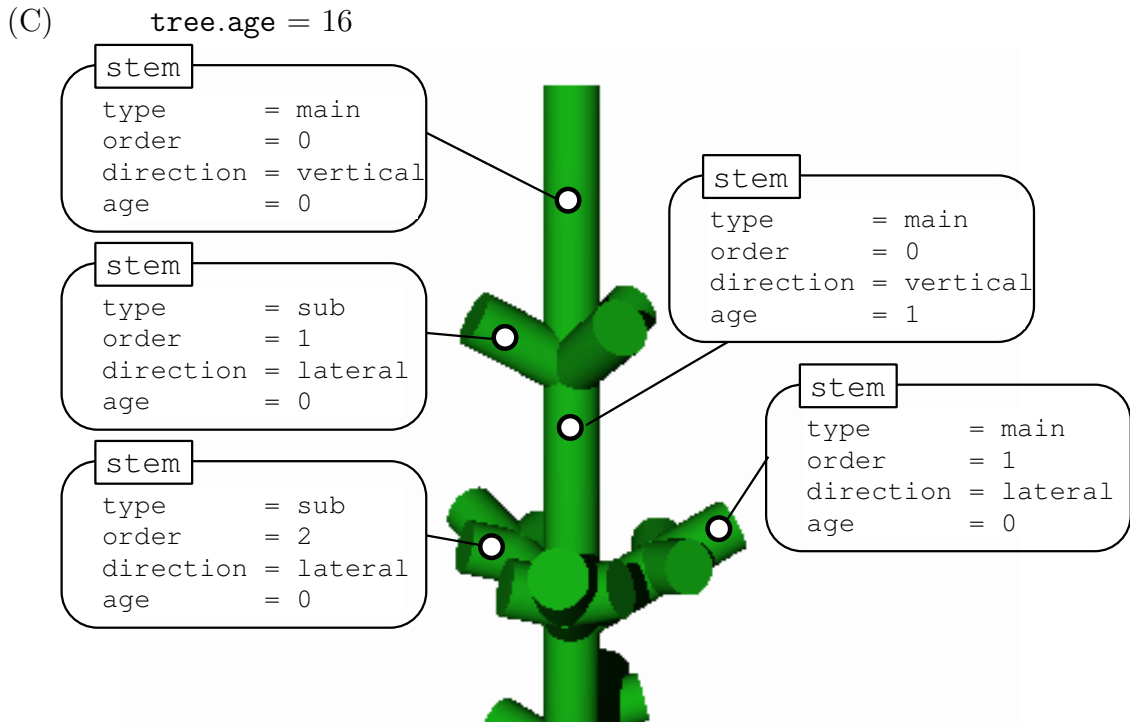


Fig. 2

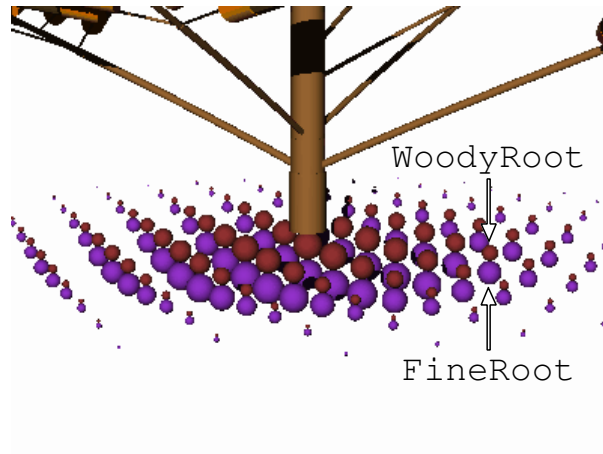


Fig. 3

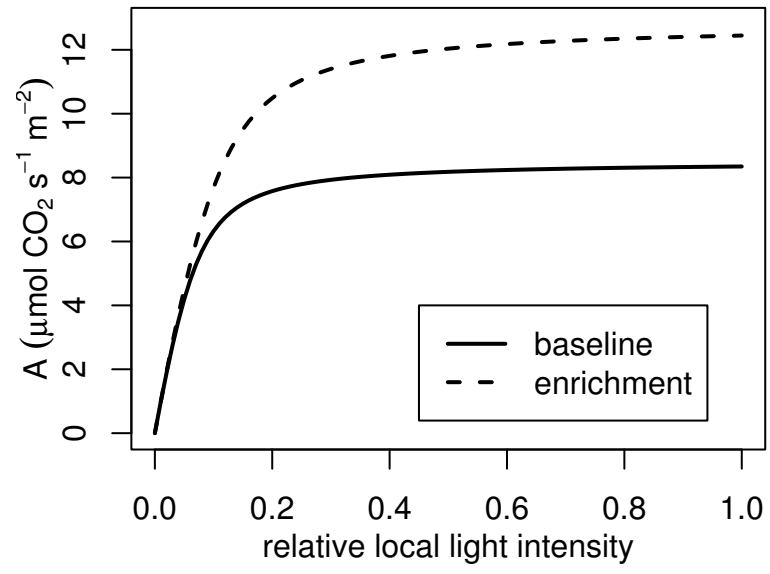


Fig. 4

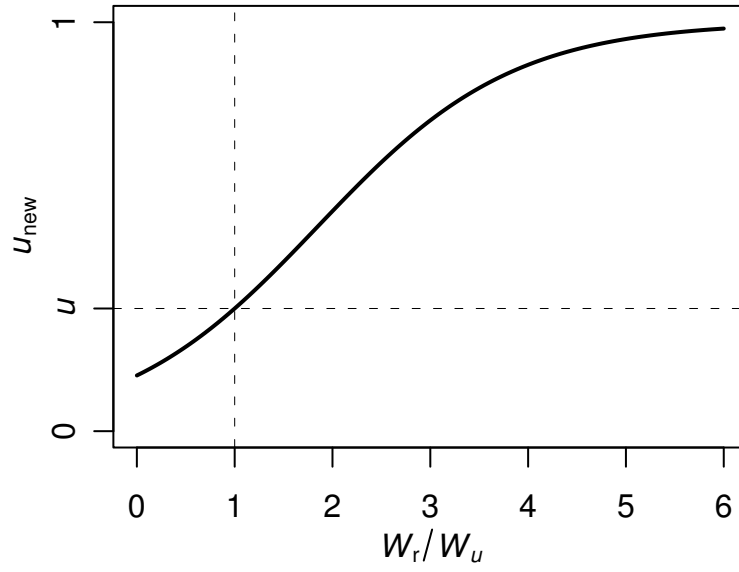


Fig. 5

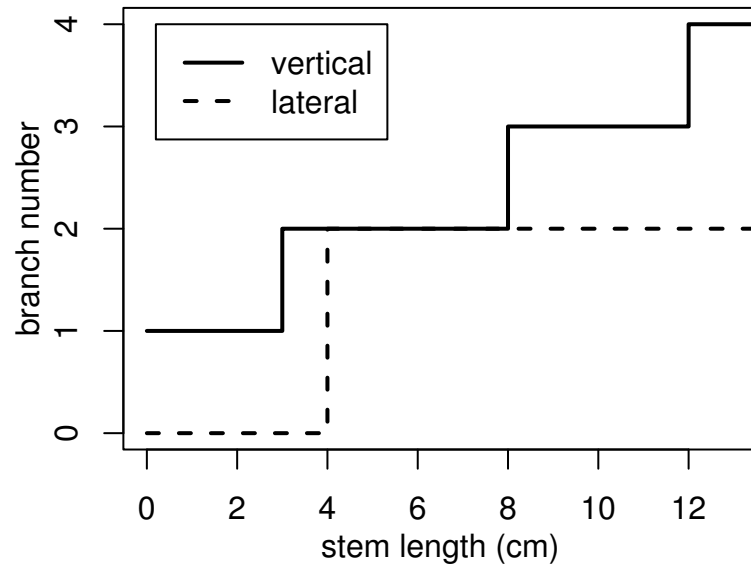


Fig. 6

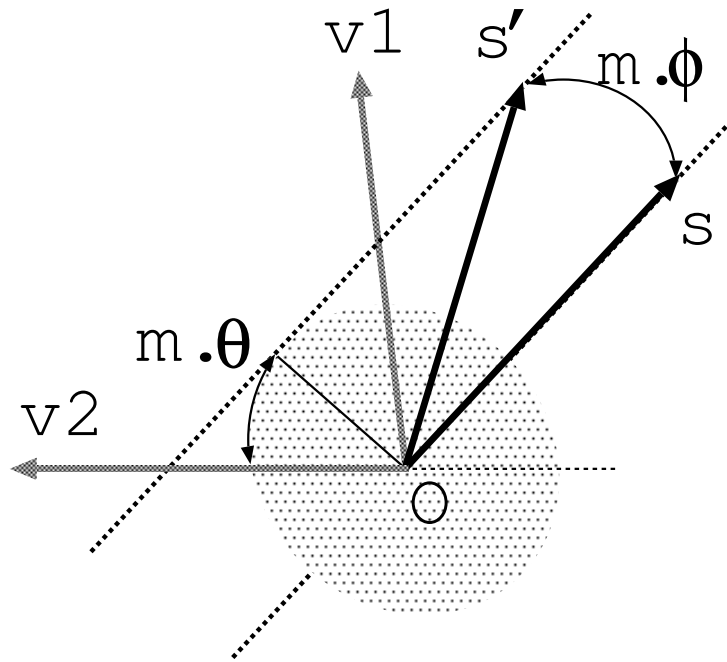


Fig. 7

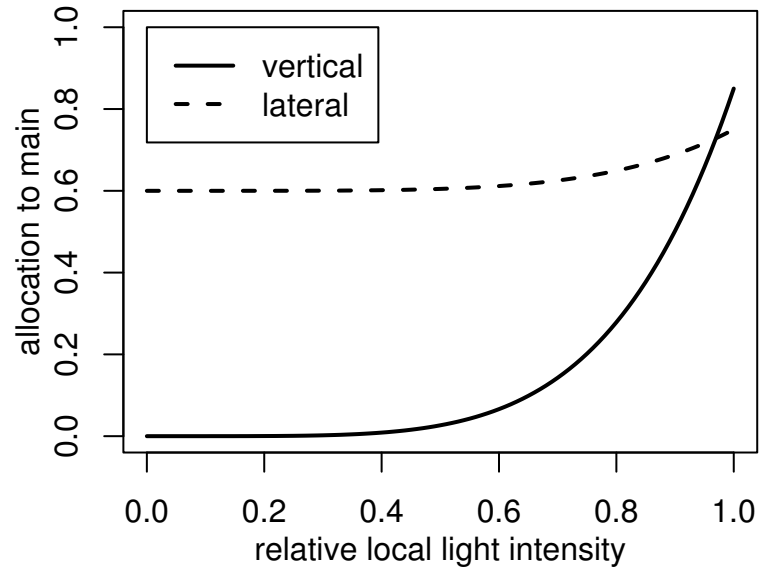


Fig. 8

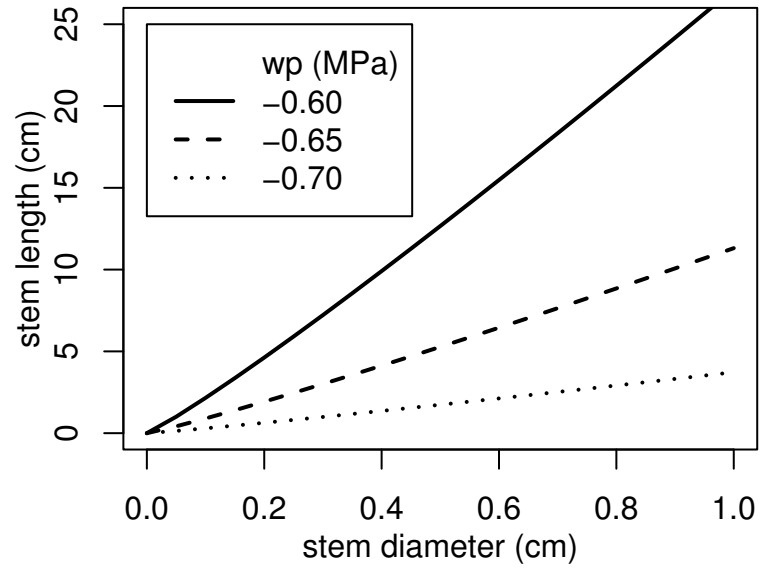


Fig. 9

(A)



(B)

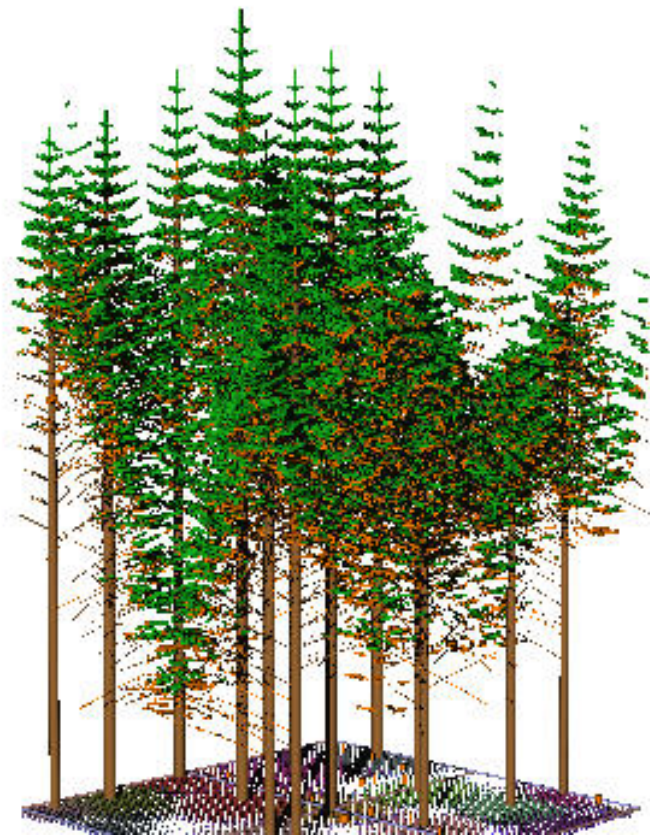


Fig. 10

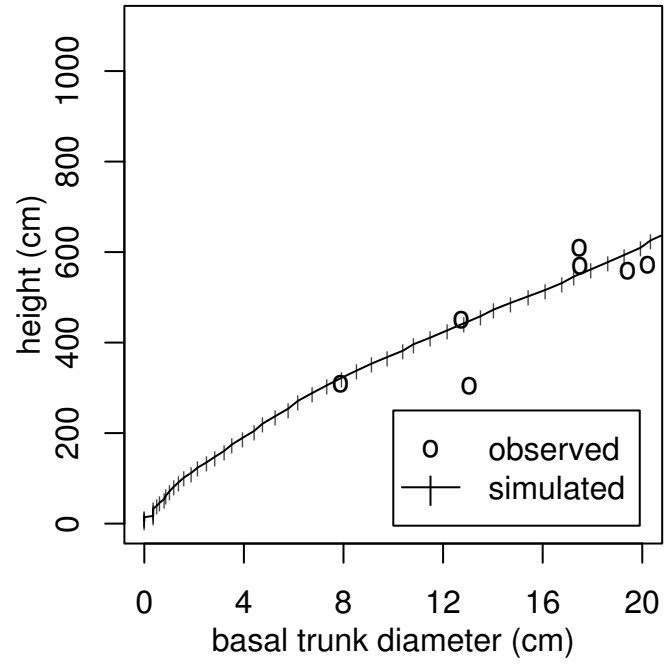
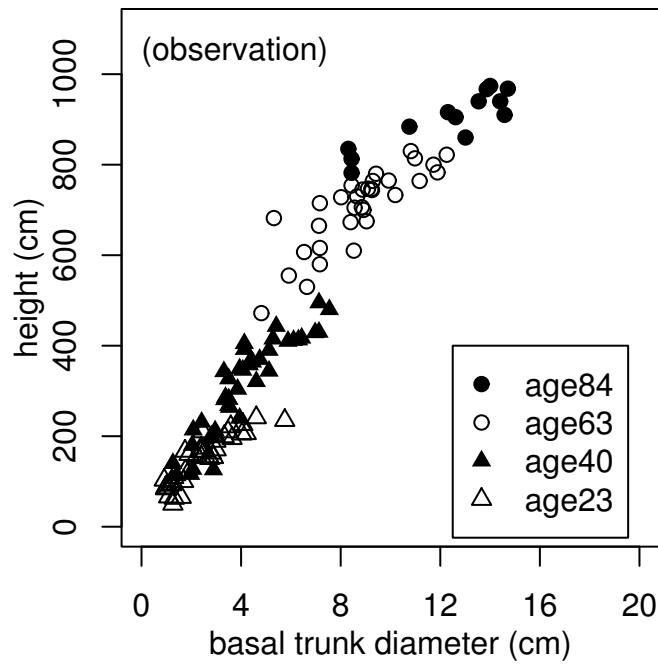


Fig. 11

(A)



(B)

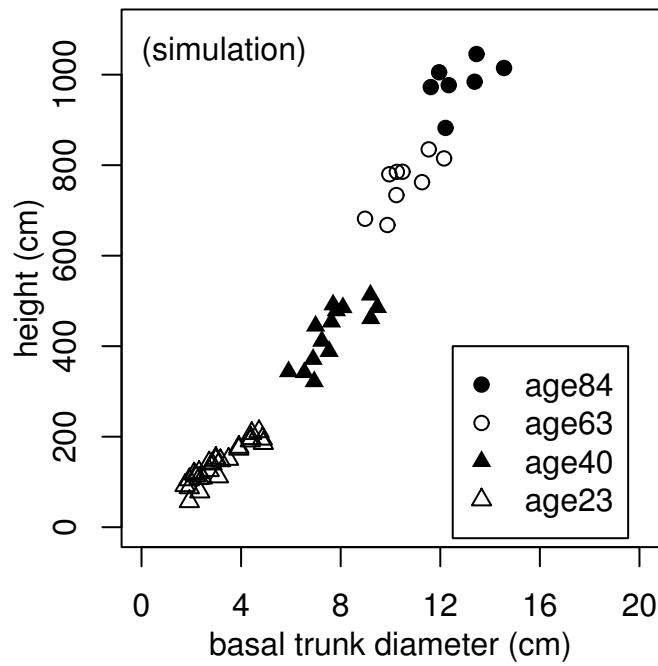
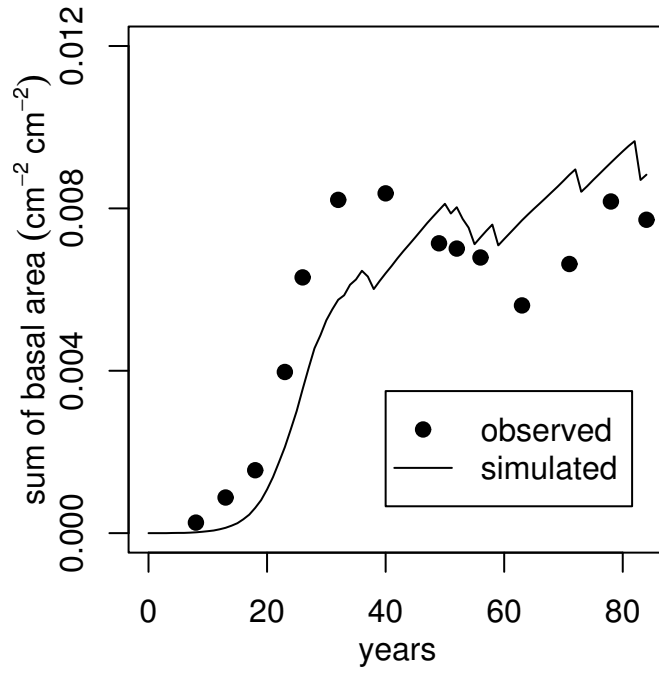


Fig. 12

(A)



(B)

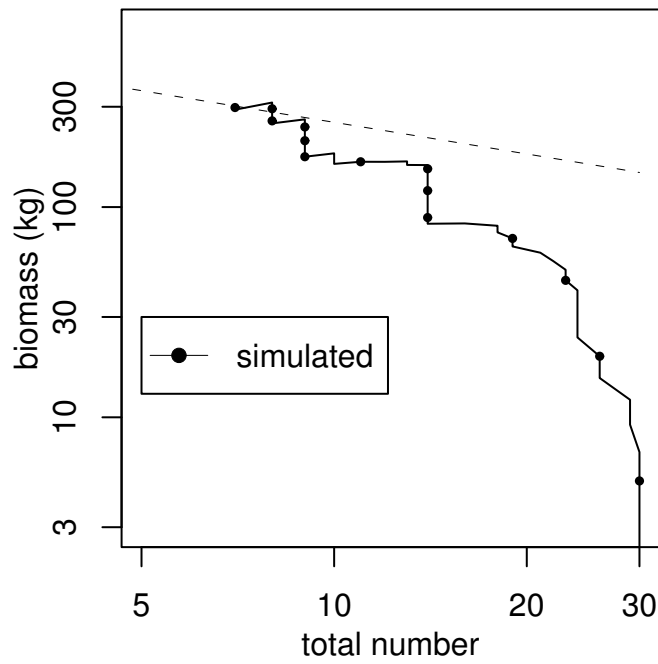
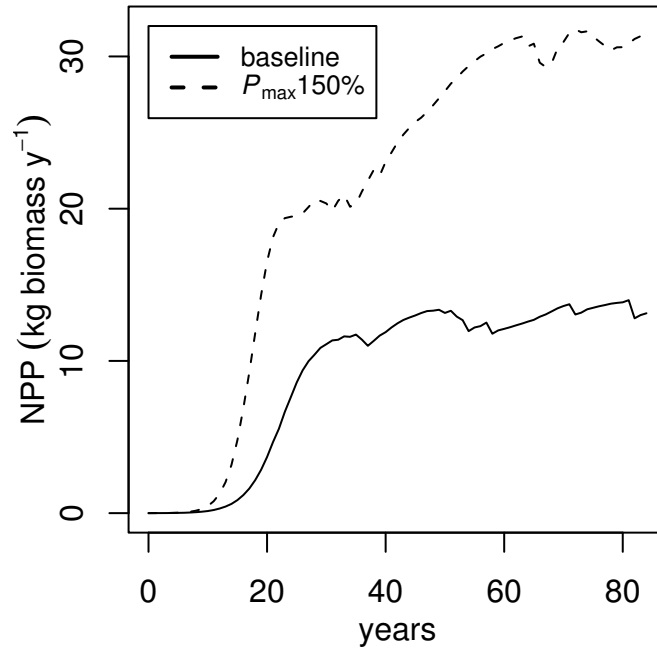


Fig. 13

(A)



(B)

